

PDZ-Reactive Peptide Activates Ephrin-B Reverse Signaling and Inhibits Neuronal Chemotaxis

Yongsheng Yu,[†] Miao Liu,[†] Tsz Tsun Ng,[‡] Feng Huang,[†] Yunyu Nie,[†] Rui Wang,[†] Zhong-Ping Yao,[‡] Zigang Li,[§] and Jiang Xia^{*,†}

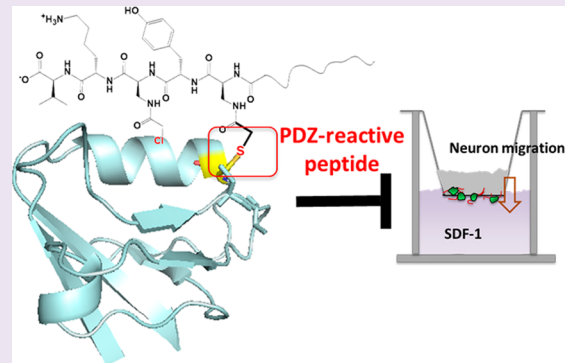
[†]Department of Chemistry, The Chinese University of Hong Kong, Shatin, Hong Kong SAR, China

[‡]Food Safety and Technology Research Centre, State Key Laboratory of Chirosciences and Department of Applied Biology and Chemical Technology, The Hong Kong Polytechnic University, Hung Hom, Kowloon, Hong Kong SAR, China

[§]Laboratory of Chemical Genomics, School of Chemical Biology and Biotechnology, Shenzhen Graduate School of Peking University, Shenzhen, 518055, China

Supporting Information

ABSTRACT: Intracellular reactions on nonenzymatic proteins that activate cellular signals are rarely found. We report one example here that a designed peptide derivative undergoes a nucleophilic reaction specifically with a cytosolic PDZ protein inside cells. This reaction led to the activation of ephrin-B reverse signaling, which subsequently inhibited SDF-1 induced neuronal chemotaxis of human neuroblastoma cells and mouse cerebellar granule neurons. Our work provides direct evidence that PDZ-RGS3 bridges ephrin-B reverse signaling and SDF-1 induced G protein signaling for the first time.



During the development of the nervous system, neuronal precursor cells are guided by extracellular cues to migrate to their precise final destinations. In vertebrates, signal transduction through the membrane-bound proteins ephrins and Eph receptors plays an essential role in regulating granule cell migration during cerebellar development.^{1,2} SDF-1 (stromal derived factor 1), a neuronal attractant expressed in the meninges, attracts neuronal precursor cells to migrate at the embryonic stage. Lu et al. found soluble EphB2-Fc inhibited granule cell chemotaxis toward SDF-1. This inhibitory effect could be blocked by the expression of a dominant negative form of PDZ-RGS3, PDZ-EGFP.³ Based on these observations, it was proposed that EphB binds ephrin-B and transduces an inhibitory signal toward neural chemotaxis through the binding interaction between the cytosolic C terminus of ephrin-B and the PDZ domain of PDZ-RGS3 (this pathway is also known as ephrin-B reverse signaling, Figure 1A).^{1,3} The mediatory role of PDZ-RGS3, however, is complicated by the promiscuity of the binding property of the ephrin-B C terminus. This sequence, which constitutes a PDZ domain binding motif, is known to bind a number of potential partners besides PDZ-RGS3.⁴ The postulation that PDZ-RGS3 is the genuine receptor of the ephrin-B C terminus that mediates the linkage between ephrin-B signaling and SDF-1 neuronal chemotaxis is mainly supported by the dominant negative mutant experiment (Figure 1B).³ In this regard, a synthetic compound that specifically and

directly acts on PDZ-RGS3 will provide explicit and direct evidence on this hypothesis.

An *in vitro* binding experiment showed that the PDZ domain of PDZ-RGS3 binds with the ephrin-B C terminus, especially the sequence QSPANIYYKV-(COOH) with a K_D around 3 μM .⁵ The solution structure of the PDZ domain shows a canonical PDZ folding, including six β -strands and two α -helices. Interestingly, this PDZ domain has three unique cysteines, Cys33, 34, and 73, at the peptide-binding site, close to -2 to -5 positions of the bound peptide (Figure 2A). Notably, the three cysteine residues are all at their free form, without forming disulfide bonds, and their side chain thiol groups point toward the peptide-binding groove. We envision that one can design peptide derivatives by installing a mild electrophilic group at selected positions of the native ligand of this PDZ domain, i.e. the ephrin-B C terminal peptide. The peptide derivative will bind to the target protein through noncovalent interaction and then react with the protein at the thiol group—hence the name “reactive peptides.” The mild electrophile only reacts with a nucleophile that is positioned adjacent to it. This “proximity-induced reactivity” effect ensures the conjugation reaction only occurs at the selected cysteine residues on the target protein. Therefore, both target selectivity

Received: August 10, 2015

Accepted: November 2, 2015

Published: November 2, 2015



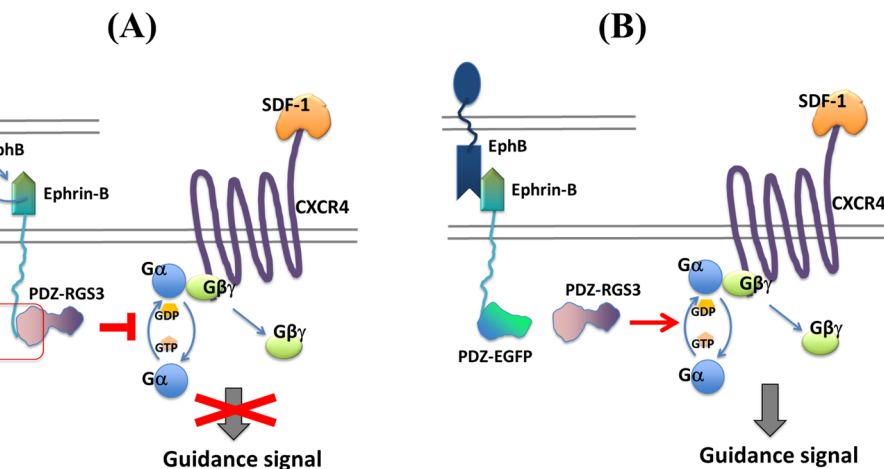


Figure 1. PDZ-RGS3, proposed to link ephrin-B reverse signaling to SDF-1 induced neuronal chemotaxis.³ (A) The mechanism of ephrin-B reverse signaling. Following the interaction of the EphB receptor and the extracellular part of ephrin-B, the binding of the cytosolic C terminus of ephrin-B with the PDZ domain of PDZ-RGS3 (shown in circle) activates the GAP activity of the RGS domain, which inhibits G-protein coupled chemotaxis induced by SDF-1 and lead to the blockage of the guidance signal. (B) A dominant negative form of PDZ-RGS3, PDZ-EGFP, competitively binds to the C terminus of ephrin-B and turns off ephrin-B reverse signals, leading to neuronal chemotaxis toward the attractant SDF-1.

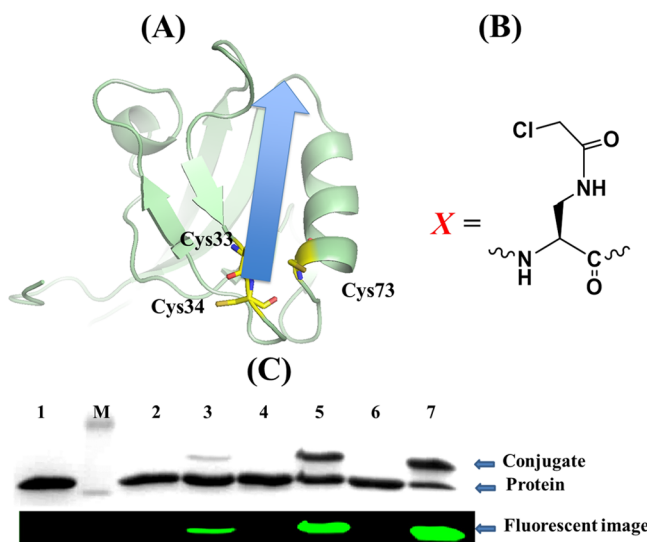


Figure 2. Structure-based design of reactive peptides for PDZ^{ΔRG3} (PDZ^{ΔRG3} denotes the PDZ domain alone of PDZ-RGS3). (A) Solution structure of PDZ^{ΔRG3} in the absence of its bound peptide shows a canonical PDZ folding and three unique cysteine residues at 33, 34, and 73 positions. The cysteine residues point to -2 to -5 positions of the putative binding peptide (PDB ID 1WHD; the blue arrow indicates the putative peptide-binding site; cysteine residues are highlighted in yellow). (B) The structure of the X residue, showing a mild electrophile chloroacetyl group to react with the nucleophilic thiol groups of the cysteines. (C) Covalent and spontaneous conjugation reaction of fluorescently labeled peptides with PDZ^{ΔRG3}. Coomassie Blue stained image (top) and fluorescent image (bottom). M, molecular weight marker; 1, PDZ^{ΔRG3} only; 2, NCB-1 + PDZ^{ΔRG3}; 3, CB-1 + PDZ^{ΔRG3}; 4, CB-2 + PDZ^{ΔRG3}; 5, CB-3 + PDZ^{ΔRG3}; 6, CB-4 + PDZ^{ΔRG3}; 7, CB-5 + PDZ^{ΔRG3}. Peptides in 5-fold excess were incubated with the PDZ protein in pH 7.4 PBS buffer for 12 h before being thermally denatured and resolved by denaturing SDS-PAGE. The gel was then imaged under a fluorescent scanner and stained by Coomassie dye.

and site specificity can be fulfilled. Our group and others have implemented this strategy for site-specific bioconjugation.^{6–13} It will be particularly valuable to develop selective and site

specific inhibitors for PDZ-peptide interactions. Because PDZ-peptide binding interactions are often weak and promiscuous, reactive peptides that covalently inhibit a single PDZ protein will achieve highly specific targeting and maximal perturbation of the signal events.¹⁴

RESULTS AND DISCUSSIONS

Design, Synthesis, and Screening of PDZ-Reactive Peptides. We designed and synthesized peptides CB-1 to CB-4 by mutating the residues at -2 to -5 positions of the ephrin-B2 PDZ binding motif (peptide NCB-1) respectively to an unnatural amino acid X (X represents a derivative of diamino-propionic acid with a chloroacetyl group at the side chain; Table 1, Figure 2B). The chloroacetyl group has been proven

Table 1. List of Peptide Derivatives

peptide names	sequence ^a
CB-1	QSPANIYXKV
CB-2	QSPANIXYKV
CB-3	QSPANXYYKV
CB-4	QSPAXIYYKV
CB-5	QSPANXYXKV
CB-6	YGRKKRRQRRR-QSPANXYXKV
NCB-1	QSPANIYYKV
NCB-2	YGRKKRRQRRR-QSPANIYYKV

^aX denotes the unnatural amino acid, (2S)-2-amino-3-[(2-chloroacetyl)amino]propanoic acid (structure shown in Figure 2B).

to be a mild nucleophile which reacts rapidly with the thiol of cysteine that is in its proximity to give a thioether bond, but its reaction with other thiol groups that are free in the solution is very slow.^{12,13} This designed local reactivity thereby ensures site specificity in bioconjugation. Here, we utilize this feature to induce site-specific covalent reaction of the peptide derivatives with the PDZ domain. We started to examine the reactivity of the synthetic peptides by simply incubating them with purified PDZ^{ΔRG3} at pH 7.4 in phosphate buffer solution. CB-3, having the electrophilic chloroacetyl group installed at the -4 position of the PDZ-binding peptide, reacted with PDZ^{ΔRG3} and

MHHHHHHSSGLEVLFQPGPSGKKLKITIRR**GKDGF**GFTIC**CDSPVR**VQAVDGGPAERAGLQQQLDTVQL
NERPVEHWK**CVELAHEIR**SCPSEIILLVWRVVVPQIK

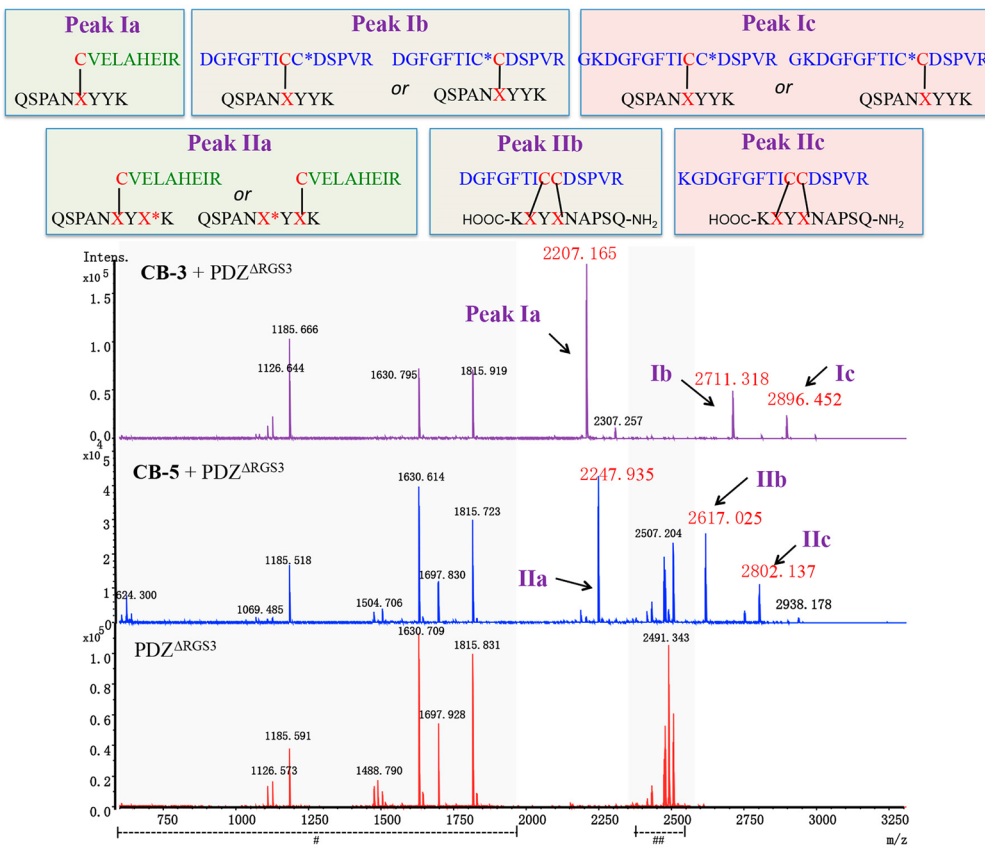


Figure 3. MALDI-TOF MS analysis of the peptide fragments in PDZ-peptide covalent conjugates and unconjugated PDZ protein. The experiment procedures are described in detail in the [Materials and Methods](#). Shown on top is the sequence of PDZ Δ RGSS 3 with the fragments containing Cys33, 34, and 73 highlighted in green and blue, and the cysteine residues in red. The assignment of major peaks is shown in Table S1 in the [Supporting Information](#). The postulated structures of the adducts of peaks Ia to IIc are shown. C* denotes cysteine residues that are modified by IAA during sample preparation. X* denotes the X residue that has reacted with mercaptoethanol during sample preparation. Two regions (m/z < 2000 and 2400–2600, # and ##) that are not critical for this analysis are marked for the best clarity and shown in detail in Figure S2 in the [Supporting Information](#).

converted 50% of the protein to the covalently linked PDZ-peptide complex. **CB-1** (with the electrophile at the -2 position) gave 18% conversion, whereas neither **CB-2** nor **CB-4** (with the electrophile at the -3 or -5 position, respectively) showed appreciable reaction products. The double mutant **CB-5** with the chloroacetyl at both -2 and -4 positions exhibited the highest reaction efficiency approaching 78% after incubation (Figure 2C).

Encouraged by the discovery of ligand-based reactive peptides toward PDZ Δ RGSS 3 , we then sought to identify which cysteine residues in PDZ Δ RGSS 3 protein act as nucleophiles in the reaction with **CB-3** and **CB-5**, and to answer the question why **CB-5** is more reactive than **CB-3**. Four cysteine residues are present in the PDZ protein: three of them, Cys33, Cys34, and Cys73, are adjacent to the peptide-binding groove, and Cys83 is located in a position far away from the peptide-binding site. We utilized trypsin digestion in conjunction with mass spectrometry to identify the reactive positions (Figure S1 in the [Supporting Information](#)). Briefly, purified PDZ Δ RGSS 3 protein was incubated with **CB-3** or **CB-5** to form a covalent complex. The protein-peptide complex was then separated from the unreacted protein by SDS-PAGE. The complex band was cut from the gel, the protein complex was digested by trypsin, and the peptide fragments were extracted from the gel and analyzed

by MALDI-TOF. Three sets of data were compared, PDZ Δ RGSS 3 alone, **CB-3+PDZ** Δ RGSS 3 and **CB-5+PDZ** Δ RGSS 3 (Figure 3). Two regions, m/z 2000 or below and m/z 2400–2600, are found to contain peptide peaks that are not related to the cysteine-containing sequences in the PDZ (Figure S2 in the [Supporting Information](#)). Specifically, three fragments generated from tryptic digestion of PDZ Δ RGSS 3 are particularly informative: two that contain Cys33 and Cys34 (namely fragment I, GKDGF, and fragment II, DGFGFTICCDSPVR) and one that contains Cys73 (fragment III, CVELAHEIR). We then looked for their covalent adducts with the reactive peptides. We identified three new peaks, Ia, Ib, and Ic, in the sample of **CB-3+PDZ** Δ RGSS 3 that did not exist in the PDZ fragments without reactive peptides. Peak Ia matches the conjugate of **CB-3** (with the C terminal valine removed by trypsin) and the fragment of the PDZ protein which contains Cys73, fragment III (theoretical m/z calculated to be 2206.785, found 2207.165). Peaks Ib and Ic correspond to the conjugates of **CB-3** (without valine) with fragments I and II of PDZ protein, respectively, which contains both Cys33 and Cys34 (Ib, calculated: 2710.916, found: 2711.318; Ic, calculated: 2896.033, found: 2896.452). Notably, one of the cysteine residues in fragments I and II, either Cys33 or Cys34, reacted with the chloroacetyl group in **CB-3**, whereas the other cysteine residue

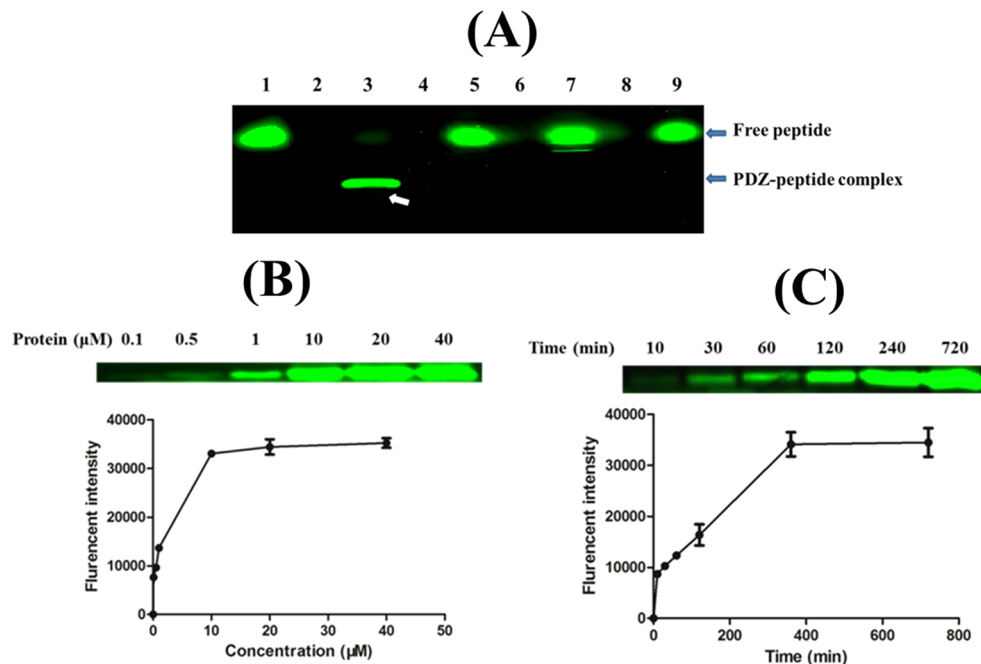


Figure 4. Covalent conjugation of reactive peptide with PDZ^{ΔRGSS3}. (A) Fluorescently labeled CB-5 only reacted with PDZ^{ΔRGSS3} (arrow) but not with other PDZ domains that contain cysteine at the peptide-binding site, InaD, GRIP1-PDZ, and TIP1^{Q43C}.¹³ CB-5 in 5-fold excess was incubated with the PDZ protein for 12 h at 37 °C before being resolved on reducing SDS-PAGE. The gel was then imaged under a fluorescent scanner. Lane 1, CB-5 peptide only; lane 2, protein PDZ^{ΔRGSS3} only; lane 3, CB-5 + PDZ^{ΔRGSS3} (covalent complex indicated by white arrow); lane 4, GRIP1 only; lane 5, CB-5 + GRIP1; lane 6, protein InaD only; lane 7, CB-5 + InaD; lane 8, protein TIP1^{Q43C} only; lane 9, CB-5 + protein TIP1^{Q43C}. (B) Product yield at different peptide/protein ratios. The concentration of fluorescent CB-5 was fixed at 80 μM, whereas the concentrations of the protein varied from 0.1 μM to 40 μM. The peptide and the protein were incubated for 12 h at 37 °C before the reactions were stopped and analyzed by SDS-PAGE. The fluorescent signals of the complexes were plotted. (C) Reaction kinetics. CB-5 in 5-fold excess was incubated with PDZ^{ΔRGSS3}, and the reaction was stopped and analyzed at various time points by SDS-PAGE.

was alkylated during sample preparation by iodoacetamide (+57.02 Da; Figure 3). We do not have sufficient data to differentiate whether Cys33 or Cys34 was responsible for the nucleophilic reaction with a chloroacetyl group in CB-3 because trypsin digestion cannot cleave between Cys33 and Cys34. Therefore, Cys73 and one of the two cysteines Cys33 or Cys34 are the reactive sites for CB-3. CB-5, on the other hand, demonstrated a different pattern. A new peptide peak, peak IIa, that corresponds to a covalent adduct through Cys73 (CB-5 without valine + fragment III; calculated: 2247.815, found: 2247.935) could be identified. In this adduct, one of the chloroacetyl groups of CB-5 has reacted with Cys73, whereas the other one has reacted with a mercaptoethanol molecule that was introduced in the sample processing step (the site of reaction in CB-5 has been marked X* in Figure 3). Interestingly, two new peaks, IIb and IIc, match the divalent covalent adducts between fragments I and II and CB-5 with the leaving of two HCl molecules (IIb, calculated: 2616.795, found: 2617.025; IIc, calculated: 2801.911, found: 2802.137; Figure 3). We reason that in these two adducts, Cys33 of the PDZ-origin peptides has conjugated with the X residue at the -2 position in CB-5 and Cys34 has reacted with the X residue at the -4 position in CB-5. The two peptides adopt an antiparallel orientation. This divalent reaction pattern explains the higher reactivity of CB-5 than CB-3. In both cases, we did not observe any covalent conjugate between Cys83 and the reactive peptides. Therefore, all three cysteine residues Cys33, 34, and 73 in the proximity of the X residues at the bound state contributed to the covalent conjugation reaction, but Cys83 did not react.

We then examined the reactivity of CB-5 with other cysteine containing PDZ proteins. No reaction was observed between CB-5 and cysteine-containing PDZ proteins, such as InaD, GRIP1-PDZ, and TIP1^{Q43C},¹³ which all contain cysteine at the peptide-binding sites (Figure 4A). Therefore, the cysteine-reactive peptide CB-5 is highly selective for PDZ^{ΔRGSS3}. Both target selectivity and site specificity observed here are consistent with the proximity-driven nature of the reaction of our initial design.^{12,13} The kinetics of reaction were also measured. At a fixed CB-5 concentration while [peptide]/[protein] ratios vary from 8:1 to 4:1 to 2:1, similar conjugation yields were observed (Figure 4B). The covalent reaction was also found to proceed rapidly with the production of the covalent adduct plateaued at 78% in 400 min (Figure 4C).

Covalent Reaction in Transfected Cells. In order to deliver the reactive peptide into the cell, a cell permeable version of the reactive peptide CB-6 was then synthesized by appending a TAT sequence to the N terminus of CB-5 (Table 1). With the assistance of a small molecule pyrenebutyrate¹⁵ (PB, 50 μM), fluorescent CB-6 entered COS-7 cells transfected with PDZ^{ΔRGSS3} and distributed into the cytosol (Figure 5A). Cells were then lysed, and the lysates were resolved by electrophoresis. A fluorescent protein band corresponding to the molecular weight of PDZ^{ΔRGSS3} was found in cells incubated with CB-6, but not in the case of nonreactive peptide NCB-2 (Figure 5B). This indicates that TAT-tagged CB-6 reacted with PDZ^{ΔRGSS3} inside the cell despite the abundant amount of cysteine-containing molecules such as glutathione in cytosol. Both peptides were then delivered to COS-7 cells that have been cotransfected with His-tagged

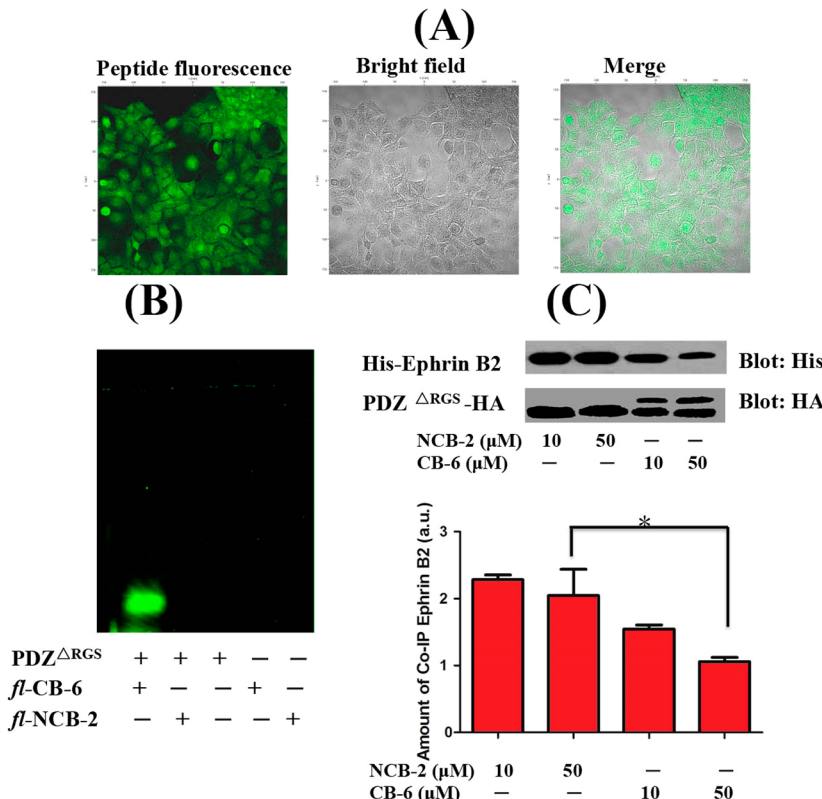


Figure 5. Reaction of CB-6 inside transfected cells. (A) Fluorescent images of cellular update of CB-6. CB-6 entered cytosol of COS-7 cells transfected with PDZ $^{\Delta RGS3}$ in the presence of PB. (B) CB-6 formed a covalent conjugate with PDZ $^{\Delta RGS3}$ inside transfected cells. CB-6 or NCB-2 were incubated with COS-7 cells transfected with PDZ $^{\Delta RGS3}$ or nontransfected cells in the presence of PB. The cells were then lysed, and the lysates were resolved on SDS-PAGE and imaged under a fluorescent imager. A band corresponds to the molecular weight of the PDZ $^{\Delta RGS3}$ -peptide adduct was observed only in CB-6 sample. (C) CB-6 effectively blocked PDZ–ephrin-B interaction in ephrin-B/PDZ $^{\Delta RGS3}$ cotransfected cells. The lower amount of the His-ephrin B2 that coprecipitated with HA-tagged PDZ protein indicates that CB-6 effectively blocks the interaction between PDZ and ephrin-B inside cells, but less efficiently by NCB-2. *p < 0.01.

intracellular fragment of ephrin-B2 and HA-tagged PDZ $^{\Delta RGS3}$. After lysis, PDZ $^{\Delta RGS3}$ was precipitated with an anti-HA antibody, and the coprecipitated ephrin-B2 was quantified by blotting with an anti-His antibody. CB-6 effectively blocked the interaction between PDZ $^{\Delta RGS3}$ and ephrin-B2, indicating that it targets the ephrin-B binding site on PDZ $^{\Delta RGS3}$ (Figure 5C). Up to 120 μ M CB-6 together with 50 μ M PB did not show significant cytotoxicity to COS-7 cells (Figure S3 in the Supporting Information). We further demonstrated the efficacy of reactive peptide in blocking protein–protein interaction inside cells by a split luciferase assay (Figure 6). When both PDZ $^{\Delta RGS3}$ -CLuc_{398–550} and NLuc_{2–416}-ephrin-B2 fusion proteins were expressed inside COS-7 cells, the binding interaction between PDZ $^{\Delta RGS3}$ and ephrin B2 induces the reassembly of CLuc_{398–550} and NLuc_{2–416} to form the functionally active luciferase, which shows a luciferin signal.¹⁶ The reactive peptide CB-6 at 10 μ M and 50 μ M could effectively suppress this signal, indicating that it can block the protein–protein interaction inside cells.

Reactive Peptide Activates Ephrin-B Reverse Signaling and Inhibits Neuronal Chemotaxis. Last, we examined whether the reactive peptide CB-6 can activate ephrin-B reverse signaling and inhibit neuronal chemotaxis toward SDF-1. Activation of ephrin-B reverse signaling was previously achieved by EphB2 and switched off by a dominant negative form of PDZ-RGS3 (Figure 1).^{3,17} Cerebellar granule neurons (CGNs) from postnatal day 5–7 C57BL/6 mice were used in a

Transwell migration assay.¹⁷ Purified CGNs migrated to the lower chamber of the Transwell attracted by SDF-1 as previously reported.¹⁷ Fluorescently labeled CB-6 entered CGNs and distributed into cytosol in the presence of PB (Figure 7A). At 10 μ M CB-6 markedly reduced the number of migrating neurons in response to SDF-1. In comparison, NCB-2 is less effective at even 50 μ M (Figure 7B and C). The same result was observed in a Transwell migration experiment using the neuroblastoma SH-SY5Y cell line, which was first shown to express PDZ-RGS3 at a high level (Figure 8). Peptide CB-6 therefore acts as an activator of ephrin-B reverse signaling and transduces the inhibitory signal to SDF-1 induced neuronal chemotaxis, similar to what EphB2-Fc does.^{3,17} Using this reactive peptide, we could directly link PDZ-RGS3 to SDF-1 neuronal chemotaxis signaling for the first time and prove the mediatory role of PDZ-RGS3 between ephrin-B reverse signaling and SDF-1 neuronal chemotaxis (Figure 9). This peptide modulator may also find application in dissecting the role of PDZ-RGS3 in axon guidance,¹⁸ chemotaxis of T cells and endothelial cells,^{19,20} long-term potentiation and synaptic maturation,^{21,22} and others.

Conclusion. The experiments above showcased how we utilized proximity-induced covalent reaction to enhance the efficacy of a peptide activator of a specific cellular signaling event. This strategy can be easily extended to other PDZ domains or even other peptide-binding domains that serve as signaling hubs, and efficient activators or inhibitors of protein–protein

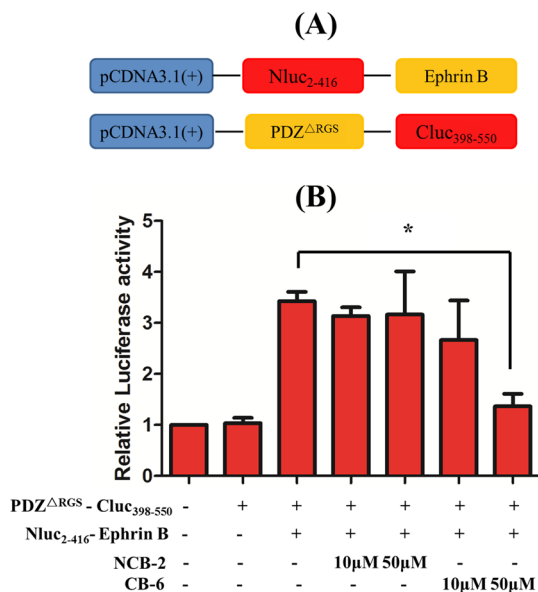


Figure 6. Inhibition of PDZ–ephrin interaction inside cells by CB-6 measured by split luciferase assay. (A) Schematic illustration of the design of split luciferase fusions. The PDZ^{ΔRGS3}–Cluc₃₉₈₋₅₅₀ and Nluc₂₋₄₁₆–ephrin-B2 fusions were cloned and inserted in mammalian expression vector pcDNA3.1(+).¹⁶ (B) CB-6 at 10 μM and 50 μM effectively blocked the interaction between PDZ and ephrin-B inside cells. Luciferase activity of transfected COS-7 cells in the presence of reversible (NCB-2) and irreversible (CB-6) peptide blockers. *p < 0.01.

interactions in cells can be devised. Although the requirement of cysteine at appropriate peptide-binding sites of the protein domain limits the number of targets this strategy can be applied to, these targets are not difficult to find, for example, 2% of PDZ domains in the Pfam database²³ have cysteine at position 33, and the percentage is 0.8% for position 34 and 1.0% for position 73. Besides finding use as specific modulators of PDZ domains, reactive peptides can also be applied as proteomic tools to accurately pull down PDZ-containing proteins. The latter study is currently underway.

MATERIALS AND METHODS

Materials. Unless otherwise noted, all reagents were purchased from commercial sources and used without further purification. Fmoc-Val-Wang resin, Rink Amide-ChemMatrix resin, and Fmoc-protected amino acids were obtained from GL Biochem Ltd. (Shanghai, China). S(6)-FAM (*f*) was purchased from Life Technologies (USA). Other reagents were purchased from commercial suppliers, including Labscan Limited (Thailand), Meryer Technologies Co., Ltd. (Shenzhen, China), Chem-Impex International Inc. (USA), and Sigma-Aldrich Co. (USA). DNA oligonucleotides were synthesized by Invitrogen (HK). Restriction endonucleases were purchased from Takara Biotech Co., Ltd. (Dalian, China). PCR products and products of restriction digests were purified by gel electrophoresis and extraction using the gel extraction kit from Takara. Plasmid DNA was purified from overnight cultures by using the Takara Plasmid Miniprep Kit. Sequencing reactions were performed and analyzed at BGI (HK). An In-Gel Tryptic Digestion Kit was purchased from Thermo Fisher Scientific (USA).

Plasmids and Antibodies. Plasmid pET.M.3C-PDZ^{ΔRGS3} (PDZ domain only, without RGS3 domain) was kindly provided by

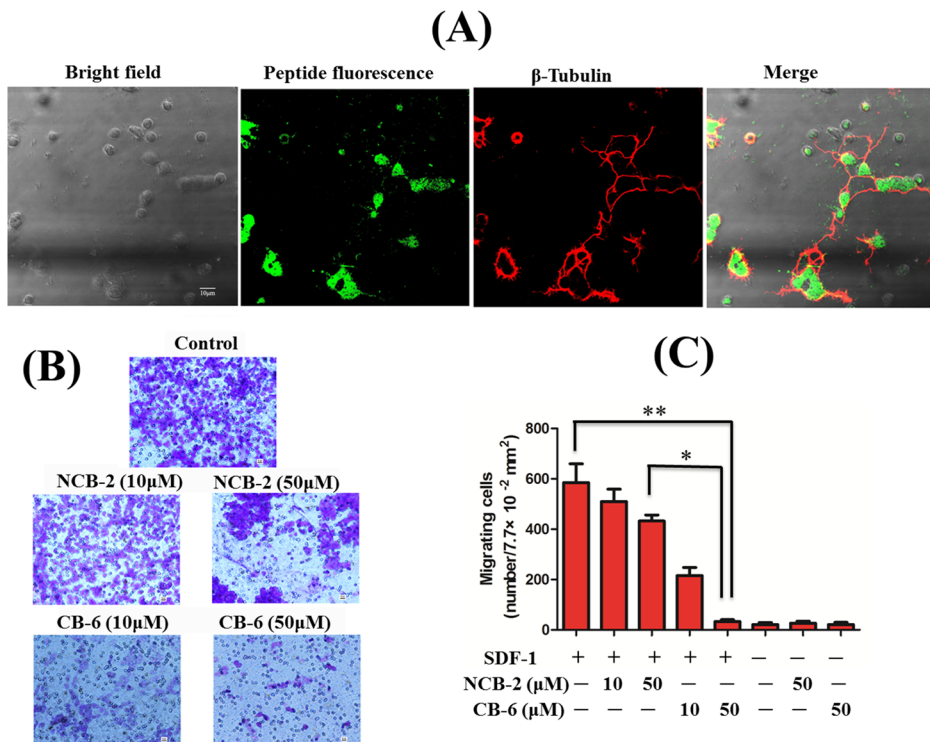


Figure 7. Effect of CB-6 on chemotaxis of neurons. (A) Fluorescent CB-6 entered the cytosol of mouse CGNs in the presence of PB. Purified CGNs from postnatal mice were cultured on coverslips and incubated with fluorescent CB-6 in the presence of PB for 15 min. The peptide was then washed away, and the cells were fixed and permeabilized following by fluorescent labeling of tubulin. The slides were imaged under a fluorescent microscope. (B) The amount of migrating neurons in response to SDF-1 markedly decreased with CB-6. Neurons were incubated in a chamber of a cell migration set up, to allow chemotaxis toward SDF-1 underneath the membrane. The cells that migrate to the bottom face of the member were fixed, labeled with crystal violet, and quantified. The more blue dots indicate more cells that migrate toward SDF-1. (C) Quantification of migrating neurons with the peptide modulators CB-6 and NCB-2 indicates CB-6 more effectively blocks SDF-1 induced neuronal migration *p < 0.01; **p < 0.001.

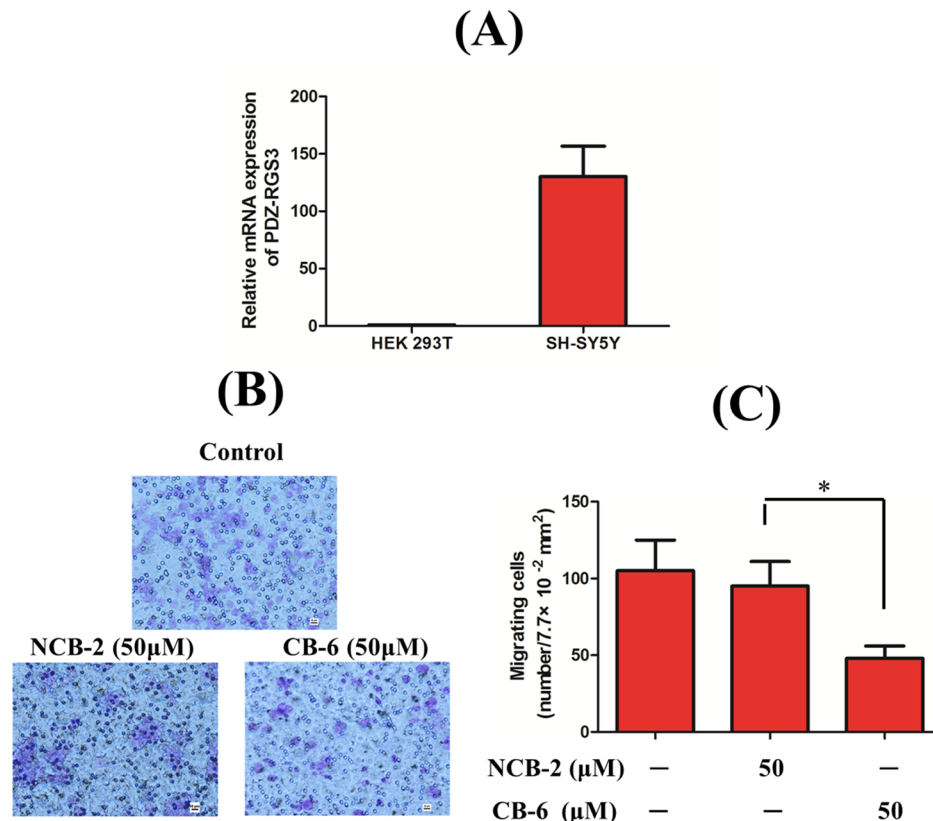


Figure 8. Effects of CB-6 on chemotaxis of SH-SY5Y cells relative to NCB-2. (A) SH-SY5Y cells express PDZ-RGS3, measured by the mRNA level of PDZ-RGS3, using another human cell line HEK293T as a control. Forward primer CAAGGAGGGTCAACCTGGACT and reverse primer GAGGTCAAGAACGGAGAAAGC were used in this experiment. (B) The amount of migrating SH-SY5Y cells in response to SDF-1 drastically decreased with CB-6. The experiments followed the same protocol as in Figure 7B. (C) Quantification of migrating cells with the peptide inhibitors indicated that CB-6 effectively blocked the SDF-1 induced migration. * $p < 0.01$.

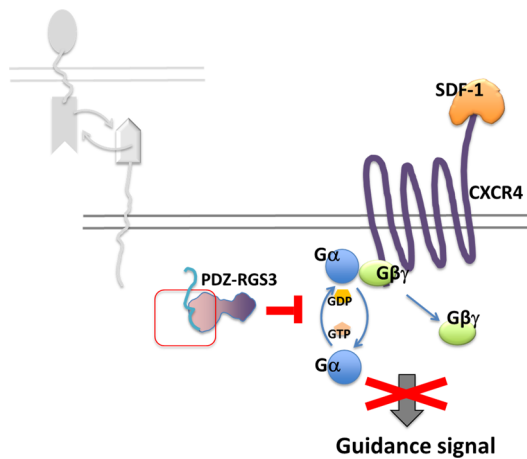


Figure 9. A schematic drawing showing that the reactive peptide (in circle) directly links PDZ-RGS3 to SDF-1 neuronal chemotaxis signaling.

Professor Mingjie Zhang (Hong Kong University of Science and Technology). The gene encoding the intracellular fragment of ephrin-B2, nucleotides 254 to 336, was synthesized by GenScript (USA). The two fragments PDZ^{ΔRG3} and ephrin B2 were inserted into plasmid pET28 (a). The initial N terminal fragments of firefly luciferase (residues 2–416, NLuc_{2–416}) and the C terminal fragment (residues 398–550, CLuc_{398–550}) were amplified from the pGL3-enhancer vector (Promega).¹⁶ Four fusion proteins, NLuc_{2–416}-ephrin B2, PDZ^{ΔRG3}-CLuc_{398–550}, His tag-ephrin B2, and PDZ^{ΔRG3}-HA tag, were generated by PCR amplification and then inserted into plasmid

pcDNA3.1(+). The primers and the restriction enzymes used in the cloning are listed in Table S2 in the Supporting Information. Anti-His tag and Anti-HA tag antibodies were purchased from Santa Cruz Biotechnology (USA). The HA-Tag IP/Co-IP Kit was purchased from Thermo Scientific (USA). Alexa Fluor 647 anti-Tubulin Beta 3 (TUBB3) was purchased from BioLegend (USA).

Cell Cultures. COS-7 cells and SH-SY5Y human neuroblastoma cells were purchased from ATCC (USA). These mammalian cells were grown in DMEM/F12 medium (Dulbecco's Modified Eagle Medium: Nutrient Mixture F-12, Life technology, USA) supplied with 10% fetal bovine serum (Life technology, USA) in a 10 cm culture dish (Corning, USA) and maintained at 37 °C in a humidified incubator supplied with 5% CO₂.

Recombinant Proteins Expression. PDZ^{ΔRG3} plasmid was transformed into *E. coli* BL21 (DE3) cells, and colonies were grown overnight at 37 °C in LB media supplemented with 100 μg/mL ampicillin or kanamycin. The starter culture was grown overnight and then was used to inoculate 600 mL of LB media supplemented with antibiotics. The cell culture was grown at 37 °C to reach OD₆₀₀ ~ 0.6 before 1 mM IPTG was added to induce protein expression. After being grown at 16 °C overnight, cells were harvested and resuspended in 30 mL of lysis buffer (containing 20 mM tris, 500 mM NaCl, 3 mM DTT, 0.1 mM PMSF, pH 7.5), sonicated, and centrifuged at 20 000g for 1 h to obtain the supernatant and to remove cell debris. Recombinant proteins were purified from lysates by Ni-NTA agarose (Qiagen) and nonspecifically bound protein removed with 10 mM imidazole in PBS. His-tagged protein was then eluted with 250 mM imidazole and dialyzed against PBS.

Peptide Synthesis and Purification. Peptides were synthesized by solid phase peptide synthesis technique based on the Fmoc/HBTU chemistry. Briefly, Fmoc protected pro-coupled resins were first deprotected by piperidine/DMF (20% v/v). Resins were then stirred

with a 5-fold excess of amino acid activated by one equivalent of 1:1 HBTU/HOBt mixture and two equivalents of DIEA in DMF. Each coupling step lasted for 30 min at RT and extensively rinsed with DMF. The Fmoc group was deprotected by piperidine/DMF (20% v/v) for 30 min and the coupling/deprotection cycles reiterated. After the peptide sequence was completed, the green fluorescent dye 5(6)-carboxyfluorescein (5(6)-FAM, *fl*) was coupled to the N terminus amino group in the presence of HBTU/HOBt. The coupling step lasted overnight at RT. For the synthesis of peptides containing the unnatural amino acid X, (2S)-2-amino-3-[[(2-chloroacetyl)amino] propanoic acid, Fmoc-Dap(Mtt)-OH was inserted in the position of amino acid displacement. The Mtt group of Fmoc-Dap(Mtt)-OH was then selectively removed with 1% TFA and 5% TIS in DCM, and chloroacetic acid was coupled in the presence of activating agents HBTU/HOBt. For peptides containing both X and N terminal fluorescent groups, selective deprotection of Mtt and coupling of the chloroacetyl side chain followed the N terminal labeling step. Peptides were cleaved from the resin by a cleavage cocktail containing TFA, EDT, water, and TIS (94:2.5:2.5:1, v/v) for 2 h at RT.

Crude peptides were then precipitated in ice-cold diethyl ether, pelleted by centrifugation, dissolved in water, purified by semi-preparative reverse phase HPLC, and lyophilized. Analytical reversed-phase HPLC was performed on a Vydac (218TP54) RP-HPLC column (C18, 5 μ m, 4.6 mm ID \times 250 mm, Alltech Associates, Inc., USA) on a LC-2010A HPLC system (Shimadzu, Japan). The identities of the synthetic peptides were confirmed by MALDI-TOF MS analysis (Figure S4 in the Supporting Information).

Protein–Peptide Covalent Conjugation Reactions. For the efficient covalent conjugation reactions, purified PDZ^{ΔRGs3} was incubated with a 5-fold excess of fluorescently labeled peptides *fl*-NCB-1, *fl*-CB-1, *fl*-CB-2, *fl*-CB-3, *fl*-CB-4, and *fl*-CB-5 in PBS at pH 7.4 for 12 h at 37 °C. To examine the specificity of the conjugation reaction, purified PDZ^{ΔRGs3}, GRIP1, InaD, and TIP1^{Q43C13} were incubated with a 5-fold excess of *fl*-CB-5 in PBS at pH 7.4 for 12 h at 37 °C, respectively. To measure the reaction kinetics, purified PDZ-RGS3 was incubated with a 5-fold excess of *fl*-CB-5 in PBS at pH 7.4 for different times (10, 30, 60, 120, 240, or 720 min) at 37 °C, respectively. To measure the conjugation reactions at different protein/peptide ratios, different concentrations (0.1, 0.5, 1, 10, 20, or 40 μ M) of purified PDZ^{ΔRGs3} was incubated with excess *fl*-CB-5 (80 μ M) in PBS at pH 7.4 for 12 h at 37 °C, respectively. The reaction solutions above were then thermally denatured in the presence of loading dye and resolved by tricine-SDS-PAGE. The gels were imaged under a Typhoon TRIO+ Variable Mode Imager (GE Healthcare, USA) for in-gel fluorescence scanning at the FITC channel. The gels were then stained by Coomassie Blue dye and imaged.

Preparation of the Samples for MS Analysis. Purified PDZ^{ΔRGs3} was incubated with a 5-fold excess of CB-3 and CB-5 in PBS at pH 7.4 for 12 h at 37 °C, respectively. The reaction solutions above were then thermally denatured in the presence of loading dye and resolved by tricine-SDS-PAGE. The gels were then stained by Coomassie Blue dye. Then a scalpel was used to excise protein bands of PDZ^{ΔRGs3} only, PDZ^{ΔRGs3}+CB-3, and PDZ^{ΔRGs3}+CB-5. Pieces were placed into a 600 μ L receiver tube. A total of 200 μ L of destaining solution was added to gel pieces, and samples were incubated at 37 °C for 30 min two times with shaking. After the gel pieces were destained, DTT was added to the tube to a final concentration of 3 mM. Samples were incubated at 60 °C for 10 min. Then iodoacetamide (IAA) was added to the samples to a final concentration of 200 mM. Samples were incubated in the dark at RT for 1 h. For the samples' digestion, gel pieces were swelled by adding 30 μ L of activated trypsin at a protease/protein ratio of 1:50 in 50 mM NH₄HCO₃ (pH 7.8). Then, the digestion mixture was removed and placed in a clean tube. To further extract peptides, 10 μ L of 1% trifluoroacetic acid was added and incubated for at 60 °C 10 min. The extraction solution was added to the digestion mixture. Then, the mixture above was detected by MALDI-MS.

MALDI-MS Analysis of the Protein Complexes. Peptide samples were mixed with equal volume of 10 mg mL⁻¹ of α -cyano-4-hydroxycinnamic acid (CHCA) in water/acetonitrile/trifluoroacetic

acid (3/7/0.01). Aliquots of 0.5 μ L of sample mixture were loaded onto an AnchorChip target plate and air-dried. Protein samples were prepared similarly, but saturated sinapinic acid was used instead of CHCA. The plate was then introduced into the mass spectrometer for MALDI-MS analysis.

An Ultraflex Xtreme MALDI-TOF/TOF mass spectrometer (Bruker Daltonics, Germany) was used for the analysis. The laser of the MALDI source was a Smart beam-II (Nd:YAG, 355 nm) pulse laser operating at a frequency of 2000 Hz. The mass spectrometer was operated in positive reflectron mode and positive linear mode for the analysis of peptides and proteins, respectively. The settings of positive reflectron mode for the ion source 1, source 2, lens, reflector 1, reflector 2, and pulsed ion extraction were 20.00 kV, 17.75 kV, 7.00 kV, 21.10 kV, 10.85 kV, and 140 ns, respectively. The sample rate and digitizer were set to 5.00GS/s. The settings of positive linear mode for the ion source 1, source 2, lens, and pulsed ion extraction were 20.00 kV, 18.80 kV, 5.60 kV, and 250 ns, respectively. The sample rate and digitizer were set to 1.25GS/s. The mass spectrometer in positive reflectron mode was calibrated with the PEG mixture (PEG600/PEG1000/PEG2000/NaI = 1/1/1/3 (w/w)). The spectral acquisition was performed using the flexControl 3.4 (Bruker Daltonics, Germany) program. The mass spectra were analyzed using flexAnalysis 3.4 and the Biotool 3.2 (Bruker Daltonics, Germany) program. The SNAP algorithm was used for peak detection.

Luciferase Activity Measurement. The split luciferase plasmids NLuc₂₋₄₁₆-ephrin-B2 and PDZ^{ΔRGs3}-CLuc₃₉₈₋₅₅₀ were constructed by following the protocol published in ref 16. COS-7 cells (2×10^5 per 35 mm dish) were transiently cotransfected with NLuc₂₋₄₁₆-ephrin-B2 and PDZ^{ΔRGs3}-CLuc₃₉₈₋₅₅₀ plasmids or a single plasmid using FuGENE HD Tranfection Reagent (Promega) according to the manufacturer's instructions. The cells were washed twice with PBS 12 h after transfection. Then the cells were first incubated with pyrenebutyrate (PB; 50 μ M) in PBS for 2 min, and then different concentrations of NCB-2 or CB-6 peptides were added, respectively. After incubation for 15 min, the cells were washed by PBS three times, and then the medium was added. Lysates were prepared using Reporter Lysis Buffer (Promega) according to the manufacturer's protocol after the peptides were incubated with cells for 48 h. For each sample, a 1:5 v/v ratio of lysate to Luciferase Assay Reagent (Promega) was added to each well. The luminescence was measured by GloMax 96 Microplate Luminometer (Promega) following the standard protocol.¹⁶

Immunoprecipitation and Western Blot. For immunoprecipitation experiments, COS-7 cells (5×10^5 per 10 mm dish) were transiently cotransfected with His tag-ephrin-B2 and PDZ^{ΔRGs3}-HA tag plasmids using FuGENE HD Tranfection Reagent (Promega) by following the manufacturer's instruction. Cells were washed twice with PBS 12 h after transfection. Then the cells were first incubated with PB (50 μ M) in PBS for 2 min, and then NCB-2 or CB-6 peptides of different concentrations were added, respectively. After being incubated for 15 min, cells were washed by PBS three times, and then the medium was added. Then, 48 h after transfection, cells were washed by PBS three times and lysed. HA-tagged PDZ^{ΔRGs3} protein was precipitated from the whole-cell lysates using HA-Tag IP/Co-IP Kit (Thermo Scientific, USA) according to the manufacturer's instruction. Recombinant anti-His monoclonal antibody (Santa Cruz) was used to quantify the amount of His-tagged ephrin-B2 fragment that coprecipitated with the PDZ^{ΔRGs3} protein by Western blotting.

C57BL/6 Mouse Granule Cell Penetration. C57BL/6 mice were purchased from the Laboratory Animal Services Centre, The Chinese University of Hong Kong. Granule cells from P5–P7 C57BL/6 mouse cerebella were dissected, dissociated, and purified as previously described with modification. The protocol including all the procedures was approved by the University Animal Experimentation Ethics Committee (AEEC) of The Chinese University of Hong Kong. Briefly, cerebella of postnatal day 5 to 7 mice were dissected and dissociated to single cell suspensions by repetitive trituration, and the cell suspension was cleared by a quick centrifugation. The cell suspension was gently loaded on a column of discontinuous Percoll gradient (35% and 60%

isotonic Percoll) and spun at 3500 rpm for 20 min. Cells at the interface between 35% and 60% Percoll layers were collected, washed, and resuspended in NB 27 medium (Life Technology). These cells were confirmed to be mostly cerebellar granule cells (CGNs) by their morphology under a microscope. Purified granule cells were incubated at 37 °C on poly-D-lysine coated glass slides to let them attach to the substratum. Fluorescently labeled peptides NCB-2 or CB-6 were added at different concentrations with 10 μM PB and incubated for 15 min. After two washes by PBS, cells were fixed with 4% paraformaldehyde for 10 min, permeabilized in 0.1% Triton for 5 min, blocked with 5% BSA for 30 min, and labeled with the tubulin-specific fluorescent antibody TUBB3 for 2 h. The slides were washed at least three times with PBS and then imaged under a confocal fluorescent microscope at the FITC channel for fluorescently labeled peptide inside cells and at TRITC channel for tubulin labeling.

Mouse CGN and SHSY-5Y Cell Migration Assay. The procedure described here is a modified version of the previously published protocol.^{3,16} Transwell membranes (polycarbonate, 5 μm pores, from Corning, USA) were precoated on both sides with laminin (20 mg mL⁻¹) for 1 h and then washed with PBS. In the low chamber, 600 μL of NB 27 growth medium containing 100 ng/mL SDF-1 (SDF-1, also called SDF-1α, was purchased from Peprotech, USA) was added. Purified mouse CGNs or SH-SY5Y neuroblastoma cells were first immobilized on a poly-D-lysine coated culture flask and incubated with NCB-2 or CB-6 peptides at different concentrations with 10 μM PB for 15 min at 37 °C. Cells were then detached from the substratum, and 1 × 10⁵ cells in 200 μL of NB 27 medium were placed in the top chamber of the Transwell and incubated at 37 °C in 5% CO₂ for 16 h to allow them to migrate to the lower side of the membrane. After incubation, cells on the membrane were first fixed by methanol and then stained by crystal violet. Cells that attached to the upper side of the membrane were wiped off, and cells that had migrated and attached to the lower side of the membrane were viewed under a microscope with a 40× objective lens. Five central fields were randomly selected for each experiment, and the cells in these fields were counted. Each condition was examined in triplicate in each experiment, and each experiment was repeated 3 to 5 times independently. Consistent quantitative results were obtained from repeated experiments.

MTT Assay. The cytotoxicity of the peptides was measured by MTT assay. COS-7 cells were treated with 50 μM PB in PBS for 10 min and then incubated with different concentrations of CB-6 in the presence of PB for 20 min. After being washed by PBS twice, the cells were incubated for 24 h in DMEM F12 containing 10% (v/v) FBS. Cell viability was then analyzed by MTT assay (MTT cell proliferation assay kit was purchased from Life Technologies, USA).

Quantitative Real-Time Polymerase Chain Reaction (RT-PCR). The expression level of PDZ-RGS3 in HEK 293T cells or SH-SY5Y cells was measured by RT-PCR. Total RNA was extracted from the HEK 293T cells or SH-SY5Y cells with Trizol reagent (Invitrogen, Carlsbad, CA) and the first-strand cDNA was reversely transcribed from RNA using the Reverse Transcription System kit (Promega, USA). RT-PCR reactions were performed using an Applied Biosystems 7500 Sequence Detection system (Applied Biosystems, USA).

ASSOCIATED CONTENT

Supporting Information

The Supporting Information is available free of charge on the ACS Publications website at DOI: [10.1021/acscchembio.5b00889](https://doi.org/10.1021/acscchembio.5b00889).

Figures S1–S4 and Table S1 and S2 ([PDF](#))

AUTHOR INFORMATION

Corresponding Author

*Phone: (852) 3943 6165. Fax: (852) 2603 5057. E-mail: jiangxia@cuhk.edu.hk.

Notes

The authors declare no competing financial interest.

ACKNOWLEDGMENTS

The authors acknowledge Éloïse Peltier for proofreading and polishing the manuscript. Financial support for this work came from the University Grants Committee of Hong Kong (ECS grant CUHK 404812, GRF grants 403711 and 404413, and AoE/M-09/12).

REFERENCES

- (1) Guan, K. L., and Rao, Y. (2003) Signalling mechanisms mediating neuronal responses to guidance cues. *Nat. Rev. Neurosci.* 4, 941–956.
- (2) Arvanitis, D., and Davy, A. (2008) Eph/ephrin signaling: networks. *Genes Dev.* 22, 416–429.
- (3) Lu, Q., Sun, E. E., Klein, R. S., and Flanagan, J. G. (2001) Ephrin-B Reverse Signaling Is Mediated by a Novel PDZ-RGS Protein and Selectively Inhibits G Protein–Coupled Chemoattraction. *Cell* 105, 69–79.
- (4) Su, Z., Xu, P., and Ni, F. (2004) Single phosphorylation of Tyr304 in the cytoplasmic tail of ephrin B2 confers high-affinity and bifunctional binding to both the SH2 domain of Grb4 and the PDZ domain of the PDZ-RGS3 protein. *Eur. J. Biochem.* 271 (271), 1725–1736.
- (5) Lin, D., Gish, G. D., Songyang, Z., and Pawson, T. (1999) The carboxyl terminus of B class ephrins constitutes a PDZ domain binding motif. *J. Biol. Chem.* 274, 3726–3733.
- (6) Chmura, A. J., Orton, M. S., and Meares, C. F. (2001) Antibodies with infinite affinity. *Proc. Natl. Acad. Sci. U. S. A.* 98, 8480–8484.
- (7) Nonaka, H., Tsukiji, S., Ojida, A., and Hamachi, I. (2007) Nonenzymatic covalent protein labeling using a reactive tag. *J. Am. Chem. Soc.* 129, 15777–15779.
- (8) Gallagher, S. S., Sable, J. E., Sheetz, M. P., and Cornish, V. W. (2009) An In Vivo covalent TMP-tag based on proximity-induced reactivity. *ACS Chem. Biol.* 4, 547–556.
- (9) Chen, Z., Popp, B. V., Bovet, C. L., and Ball, Z. T. (2011) Site-specific protein modification with a dirhodium metallocpeptide catalyst. *ACS Chem. Biol.* 6, 920–925.
- (10) Holm, L., Moody, P., and Howarth, M. (2009) Electrophilic affibodies forming covalent bonds to protein targets. *J. Biol. Chem.* 284, 32906–32913.
- (11) Gushwa, N. N., Kang, S., Chen, J., and Taunton, J. (2012) Selective targeting of distinct active site nucleophiles by irreversible Src-family kinase inhibitors. *J. Am. Chem. Soc.* 134, 20214–20217.
- (12) Wang, J., Yu, Y., and Xia, J. (2014) Short peptide tag for covalent protein labeling based on coiled coils. *Bioconjugate Chem.* 25, 178–187.
- (13) Lu, Y., Huang, F., Wang, J., and Xia, J. (2014) Affinity-guided covalent conjugation reactions based on PDZ-peptide and SH3-peptide interactions. *Bioconjugate Chem.* 25, 989–999.
- (14) Fujii, N., Haresco, J. J., Novak, K. A., Stokoe, D., Kuntz, I. D., and Guy, R. K. (2003) A selective irreversible inhibitor targeting a PDZ protein interaction domain. *J. Am. Chem. Soc.* 125, 12074–12075.
- (15) Takeuchi, T., Kosuge, M., Tadokoro, A., Sugiura, Y., Nishi, M., Kawata, M., Sakai, N., Matile, S., and Futaki, S. (2006) Direct and rapid cytosolic delivery using cell-penetrating peptides mediated by pyrenebutyrate. *ACS Chem. Biol.* 1, 299–303.
- (16) Yu, Y., Wang, J., Liu, J., Ling, D., and Xia, J. (2015) Functional assembly of protein fragments induced by spatial confinement. *PLoS One* 10, e0122101.
- (17) Lu, Q., Sun, E. E., and Flanagan, J. G. (2004) Analysis of PDZ-RGS3 function in ephrin-B reverse signaling. *Methods Enzymol.* 390, 120–128.
- (18) Bush, J. O., and Soriano, P. (2009) Ephrin-B1 regulates axon guidance by reverse signaling through a PDZ-dependent mechanism. *Genes Dev.* 23, 1586–99.
- (19) Sharfe, N., Freywald, A., Toro, A., Dadi, H., and Roifman, C. (2002) Ephrin stimulation modulates T cell chemotaxis. *Eur. J. Immunol.* 32, 3745–3755.
- (20) Salvucci, O., de la Luz Sierra, M., Martina, J. A., McCormick, P. J., and Tosato, G. (2006) Eph-B2 and Eph-B4 receptors forward

signaling promotes SDF-1-induced endothelial cell chemotaxis and branching remodeling. *Blood* 108, 2914–2922.

(21) Armstrong, J. N., Saganich, M. J., Xu, N. J., Henkemeyer, M., Heinemann, S. F., and Contractor, A. (2006) B-ephrin reverse signaling is required for NMDA-independent long-term potentiation of mossy fibers in the hippocampus. *J. Neurosci.* 26, 3474–3481.

(22) Lim, B. K., Matsuda, N., and Poo, M. M. (2008) Ephrin-B reverse signaling promotes structural and functional synaptic maturation in vivo. *Nat. Neurosci.* 11, 160–169.

(23) Finn, R. D., Bateman, A., Clements, J., Coggill, P., Eberhardt, R. Y., Eddy, S. R., Heger, A., Hetherington, K., Holm, L., Mistry, J., Sonnhammer, E. L. L., Tate, J., and Punta, M. (2014) Pfam: the protein families database. *Nucleic Acids Res.* 42, D222–D230.